

Silver migration at the Ag|Sm_{0.2}Ce_{0.8}O_{1.9} interface

Magdalena Maria Dudek · Michał Mosialek ·
Paweł Nowak · Joanna Wojewoda-Budka ·
Manuela Reben

Received: 18 December 2013 / Revised: 30 April 2014 / Accepted: 3 May 2014 / Published online: 22 May 2014
© The Author(s) 2014. This article is published with open access at Springerlink.com

Abstract The behavior of a silver electrode contacting Ce_{0.8}Sm_{0.2}O_{1.9} (samaria-doped ceria or SDC) electrolyte under external cathodic polarization in the temperature range 350–700 °C was examined by means of long-term polarization experiments, scanning electron microscopy, and electrochemical impedance spectroscopy. A silver deposit is formed around the silver cathode via a surface migration mechanism without the occurrence of the gas-phase transport phenomenon during polarization. This results in an increase in both the electrode-electrolyte contact area and the triple-phase boundary length, which in turn causes decreases in charge transfer resistance and electrolyte resistance.

Introduction

Research in the field of solid oxide fuel cells (SOFC) is focused nowadays on developing materials suitable for work at an intermediate temperature range (500–700 °C). However, lowering temperatures causes an increase in polarization losses on the cathode. One of the methods used to improve the performance of oxide cathodes is the addition of noble metals. Silver shows the best catalytic activity in the oxygen reduction

reaction (ORR) [1], while its price is the lowest among the noble metals. Several composite materials containing silver and oxide cathode material, such as La_{0.6}Sr_{0.4}Co_{0.2}Fe_{0.8}O₃, La_{0.8}Sr_{0.2}MnO₃ (LSM), Sm_{0.5}Sr_{0.5}CoO_{3-δ}, La_{1.6}Sr_{0.4}NiO₄, Ba_{0.5}Sr_{0.5}Co_{0.6}Fe_{0.4}O_{3-δ}, or Ba_{0.5}Sr_{0.5}Co_{0.8}Fe_{0.2}O_{3-δ} (BSCF), exhibit much better electrochemical performance than pure oxide material [2–12]. Silver is also used for the construction of current collectors and as a sealant. Guo et al. [13] showed that the presence of silver in a current collector had a positive influence on ORR at a BSCF cathode. Su et al. [10] showed that the presence of as little as 2 % Ag significantly reduced the resistance of the electrode and enhanced its catalytic performance in ORR. The disadvantages of silver are a low melting point, high volatility, and susceptibility to migration in the electric field [5, 14–20]. The problems of volatility and electromigration should become less important at a lower temperature range. Jaiswal and Wachsman [14] reported Ag migration at 625 °C under 250 mA bias, leading to depletion of the composite cathode of silver and silver deposition on the surface of the electrolyte. In a similar experiment, performed at 500 °C, they observed no changes in the composite electrode structure. Sasaki et al. [21] showed that a composite cathode, Ag–Sc_{0.10}Ce_{0.01}Zr_{0.89}O₂, did not change upon prolonged polarization at –0.5 V at a temperature of 500 °C.

A quasi-point electrode is a powerful tool to study ORR [1, 22, 23] and the migration of noble metals [5, 17–20] due to its simplified geometry. Jacobsen et al. [24, 25] examined a platinum quasi-point electrode contacting an yttria-stabilized zirconia (YSZ) electrolyte. They reported a decrease (up to two orders of magnitude) in the impedance of the platinum electrode after polarization. This decrease continued for a considerable time. An explanation of this phenomenon was given by Nielsen and Jacobsen [17, 18], who found metal deposits around quasi-point metal electrodes following negative polarization at 1,000 °C for Pt and Pd and at 920 °C for silver. As the mechanism of those changes, they suggested

M. M. Dudek (✉)
Faculty of Fuels and Energy, AGH-University of Science and
Technology, Mickiewicza 30, 30-059 Cracow, Poland
e-mail: potoczek@agh.edu.pl

M. Mosialek · P. Nowak
Jerzy Haber Institute of Catalysis and Surface Chemistry PAS,
Niezapominajek 8, 30-239 Cracow, Poland

J. Wojewoda-Budka
Institute of Metallurgy and Materials Science PAS, Reymonta 25,
Cracow, Poland

M. Reben
Faculty of Materials Science and Ceramics, AGH-University of
Science and Technology, Mickiewicza 30, 30-059 Cracow, Poland

sublimation in the case of platinum and silver electrodes and surface transport in the case of palladium electrodes. The migration of silver at 600 °C and −0.5 V at the Ag|YSZ and Ag|Gd_{0.2}Ce_{0.8}O_{1.9} interfaces has been reported in papers by Mosialek et al. [19, 20], in which the formation of silver deposits with diameters up to 5 mm was observed around quasi-point Ag electrodes after long polarization (up to 18 h). Also, our preliminary results [5] showed that even a brief (10 min) polarization caused significant changes in the impedance of a silver electrode contacting the samaria-doped ceria (SDC) electrolyte. The observed mobility of silver at the silver/solid electrolyte interface may cause problems in the application of silver as a cathode in fuel cells. The goal of this study was to explore ranges of temperatures and potentials applicable in fuel cells in order to find a particular range where this disadvantageous phenomenon does not occur. It would seem that the mobility of silver should be less significant at low temperatures. Therefore, SDC was chosen as an electrolyte because it can be used at relatively low temperatures.

Experimental

The SDC electrolytes were prepared as described in [26]. Wires made of 99.99 % silver, with a diameter of 0.5 mm, were supplied by Mennica Polska S.A. La_{0.6}Sr_{0.4}Co_{0.2}Fe_{0.8}O_{3-δ} (LSCF) paste (Fuel Cell Materials) was screen-printed onto the SDC surface, which was then fired for 2 h at 1,100 °C with a heating and cooling rate of 1 °C min^{−1}. The set-up for electrochemical measurements was described previously [27]. Polarization experiments of long duration were performed using the Gamry 300 series potentiostat/galvanostat/ZRA and software written for chronoamperometry. All experiments were performed in stagnant air. First, the cell was heated to the predetermined temperature, and the electrode was left at the open-circuit potential to stabilize (usually 30 min). During this time, several impedance spectra were recorded consecutively to check the stability of the electrode. Then the potential was set to the selected value (between −0.005 and −0.5 V vs. the silver reference electrode), and the current was recorded for a predetermined time (up to 60 h, depending on potential and temperature). At the end of the experiment, the heat was switched off, and the system was allowed to cool with the electrode under polarization. Afterwards, SEM examination of the cold electrodes and the electrolyte surface was performed. Impedance spectra were recorded continuously for selected combinations of temperature and potential during polarization at the predetermined time intervals. The frequency range used in the electrochemical impedance spectroscopy (EIS) measurements was from 0.1 or 1 Hz to 300 kHz. The amplitude of the sinusoidal voltage signal was 5 mV. For the analysis of the impedance data, the MINUIT program [28], based on a complex non-linear regression least-square fitting procedure, was used.

The scanning electron microscope XL30 ESEM (FEI), equipped with an X EDAX GEMINI 4000 system, was used for the study of the morphology as well as for microanalysis of the samples.

To determine the impact of temperature only on the behavior of the investigated Ag|SDC system, a number of reference experiments without polarization were performed.

In this study, hot-stage microscopy was used to visually follow the thermal changes and interactions between Ag and SDC. The measurement was performed with the use of a Leitz type II microscope equipped with a CCD camera in an air atmosphere, from room temperature up to 1,200 °C at the heating rate of 3 °C min^{−1}. The images were recorded in steps of 10 °C. Temperature measurement error was ±5 °C. A ball-shaped sample of Ag was placed on the polished surface of the SDC disk; then the components were placed on an alundum holder inside the furnace.

Results

The influence of temperature on the Ag|SDC interface

Determination of the interaction between the two components, i.e., the Ag point electrode and SDC electrolyte, was made by means of the HSM (Fig. 1). The HSM observations indicate that the interaction between the Ag point electrode and SDC disk started at about 370 °C, as manifested by a slight bulge at the SDC electrolyte surface in contact with the Ag sample. The size and the shape of the Ag sample as well as the contact area of two components remained unchanged until the temperature range of 890–895 °C was reached. In this temperature range, expansion of the contact area between the base and the Ag ball was observed (Fig. 1c, d). The temperature 920 °C was determined as the melting point of the Ag sample, at which the electrode changed its shape from circular to semicircular (Fig. 1f).

Scanning electron microscopy observation was also performed for the reference Ag|SDC system without polarization within the same temperature range. No silver deposit was observed around the silver cathode without polarization. Only some small silver particles on the SDC sample were observed as contamination under scanning electron microscopy, especially at temperatures above 600 °C (Fig. 2), probably due to silver evaporation.

The influence of temperature and potential on the growth of silver deposits

Setting the electrode to the negative potential resulted in a continuous increase in current (Fig. 3). After the experiment, a silver deposit was invariably observed around the cathode. The increase in current was observed at all temperatures and overpotentials, even as low as 350 °C and 5 mV, respectively; however, at low temperatures or overpotentials, in the initial period, the current first increased, then decreased, then began to increase continuously.

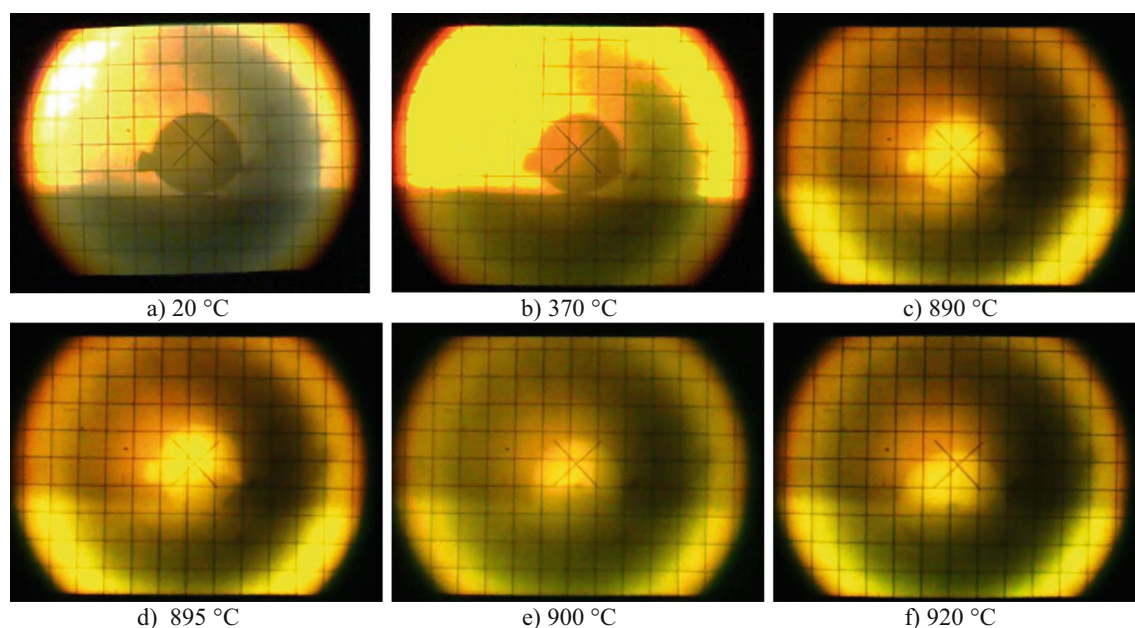


Fig. 1 Interaction behavior of Ag point electrode and SDC electrolyte using hot-stage microscopy: **a** initial condition, 20 °C; **b** beginning of the interaction, 370 °C; **c, d** an increase in contact area, 890–895 °C; **e** onset of melting, 900 °C; and **f** melting point of Ag, 920 °C

The greater the current flow in the experiments performed at higher temperatures and greater negative potentials, the larger the silver deposits formed on the electrolyte surface. The obvious reason for the increase in current was the formation of the silver deposit (Fig. 4), which increased both the contact area between the silver electrode and the electrolyte as well as the three-phase boundary (tpb) length, which, in turn, caused the increase in current. Despite similar conditions, the shape of the current-potential curve differed from experiment to experiment. One of the possible reasons for the non-

reproducibility of the course of current over time is the non-reproducibility of the initial area of contact between the silver electrode and the electrolyte.

The silver deposits that formed around the location where the cathode contacted the electrolyte are presented in Fig. 4. The electrolyte surface at the location where the polarized electrode contacted the electrolyte and surrounding area can be divided into five typical regions (see Figs. 4 and 5). Inner region 1 corresponds to the location where the electrode contacted the electrolyte. When the electrode was removed after the experiment performed at the higher temperatures (500–700 °C), small pieces of electrolyte were removed together with the electrode, and a hole in the electrolyte, not observed at lower temperatures (350–400 °C), became visible (Figs. 4a, b and 5a, b). At this location, energy dispersive X-ray (EDX) analysis (see Table 1) showed the elemental composition typical for the electrolyte (no silver present). In the region marked 2, silver covered the surface of the electrolyte with a dense deposit. The silver deposit was composed of grains with diameters of a few micrometers, closely covering the surface. Isolated holes in this silver deposit appeared in region 3, exposing the electrolyte surface (Fig. 5c). Region 4 (Fig. 5d) consisted of elongated silver islands forming a network on the electrolyte surface. Their thickness varied from 0.5 to 1.2 μm (see the cross-section in the inset in Fig. 5d). Finally, isolated small silver islands, either circular or irregular in shape, were scattered over region 5 (Fig. 5e).

In order to define the minimum value of negative polarization which causes silver migration, a series of experiments at 600 °C was performed using smaller and smaller negative potentials (−0.5, −0.2, −0.1, −0.05, −0.02, −0.005). The

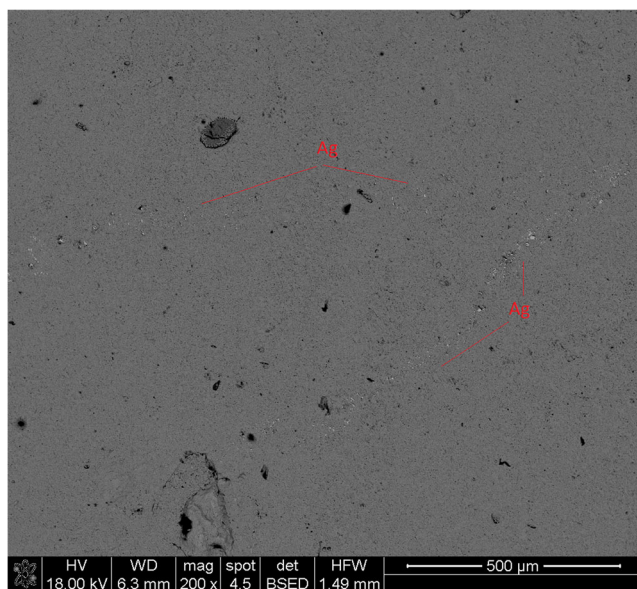


Fig. 2 SEM image of SDC surface electrolyte involving Ag particles deposited without polarization

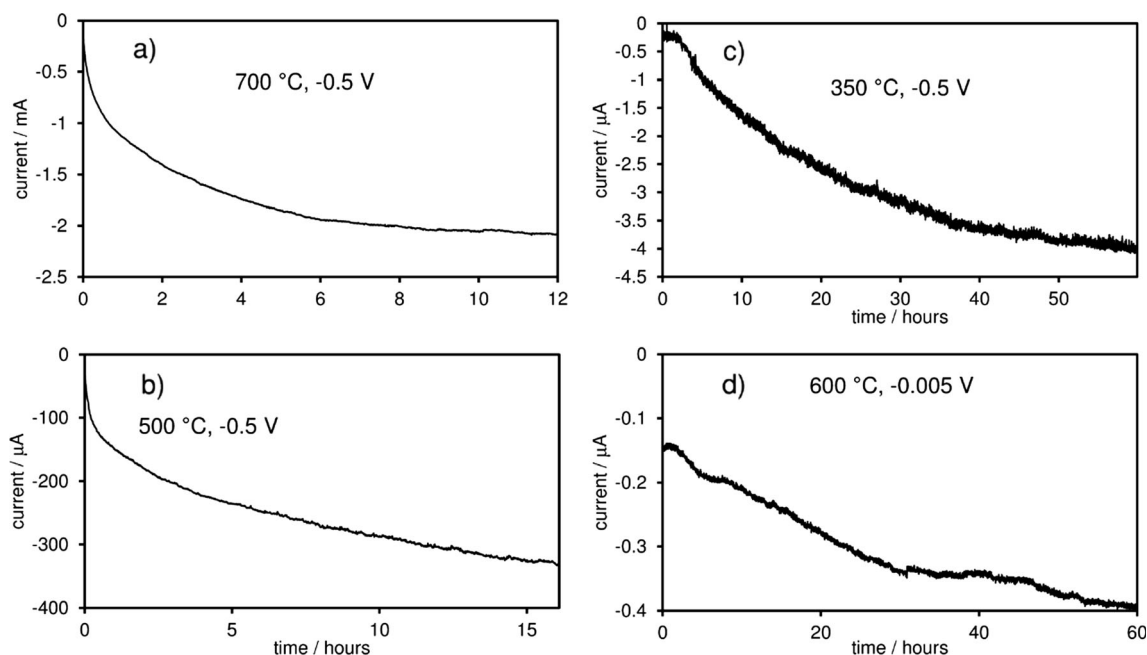


Fig. 3 Current recorded during the long-term polarization experiments performed under different experimental conditions: **a** 700 °C/−0.5 V; **b** 500 °C/−0.5 V; **c** 350 °C/−0.5 V; and **d** 600 °C/−0.005 V. The curves were smoothed by averaging over a period of 20 s

results of the experiment at −0.005 V are presented in Figs. 3d and 4d. It can be seen that even such slight negative polarization induced a continuous increase in current. At the same time, a subtle silver deposit was observed around the electrode.

Electrochemical impedance spectroscopy experiments

Examples of EIS spectra recorded during the polarization of the silver electrode at different temperatures, potentials, and times of polarization are presented in Fig. 6. The equivalent electrical circuit (EEC) applied for the interpretation of the spectra registered at the temperature 700 °C (Fig. 7a) consists of the resistance of the electrolyte (R_0), the resistance of the reaction (R_1), and the constant phase element (CPE), whose impedance may be expressed by the following equation [29, 30]:

$$Z_{CPE} = \frac{1}{2\pi f_0 C_0} \left(\frac{f_0}{jf} \right)^\alpha \quad (1)$$

where f is the frequency, f_0 is the frequency of reference (assumed at 1,000 Hz), C_0 is the capacitance at the frequency of reference, and α is a coefficient close to 1 for an ideal capacitor and usually assuming a value between 0.7 and 1.0 in the case of non-ideal capacitance. The same CPE element may represent the diffusional (Warburg) impedance, but the coefficient α in this case is 0.5. All of the spectra registered at the temperature 700 °C have the shape of a depressed semicircle.

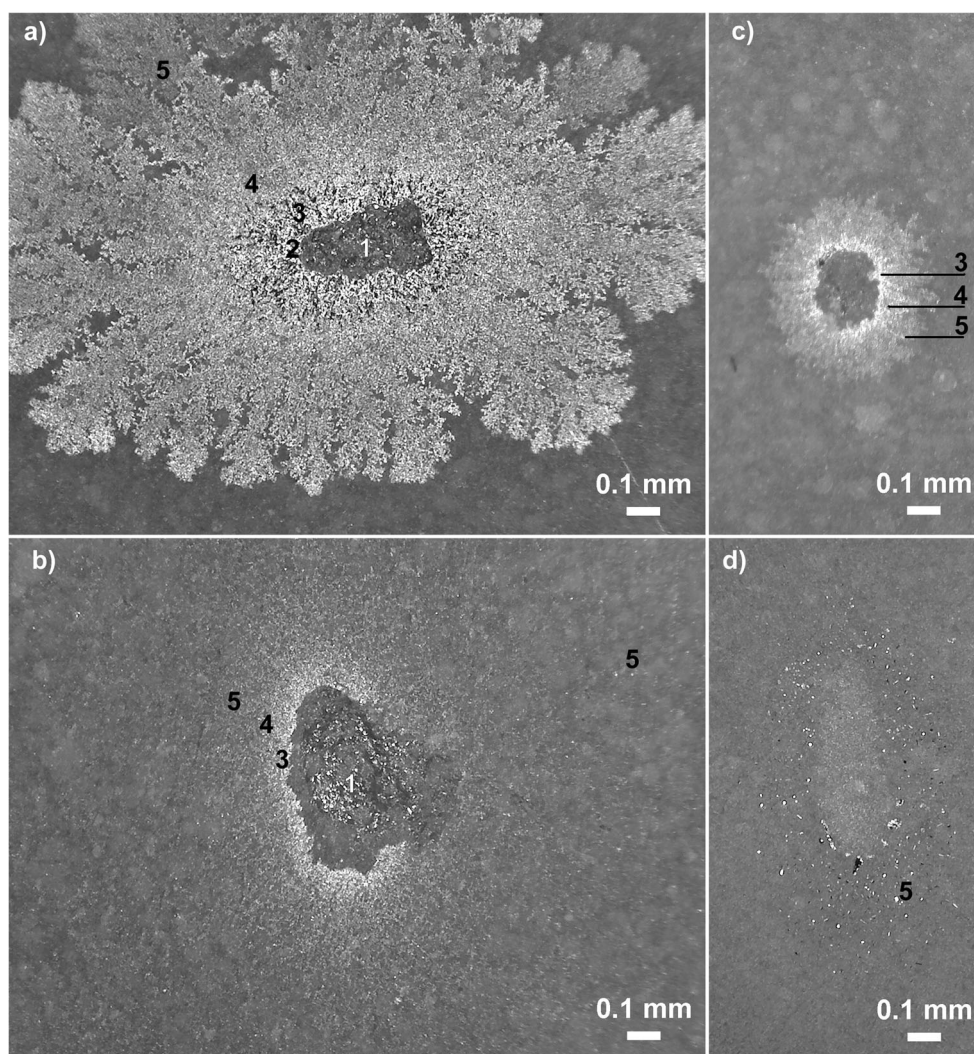
In all cases, it was possible to fit the impedance data with the equation describing the EEC from Fig. 7a, except for the first spectrum, which was significantly distorted due to rapid changes in electrode impedance over time at the beginning of the experiment. The quality of the fit was characterized by the standard deviation s , calculated from the following equation:

$$s = \sqrt{\frac{\sum_{i=1}^n \left(\frac{\text{Modulus}(Z_{i,\text{measured}} - Z_{i,\text{fitted}})}{\text{Modulus}(Z_{i,\text{measured}})} \right)^2}{n-1}} \quad (2)$$

where Z_i is the impedance at the frequency number i , and n is the number of frequencies in the impedance spectrum. In all cases, the standard deviation was below 0.01, which means that the assumed EEC describes the measured data well. The quality of fit may be also inferred by visual inspection from Fig. 8, where the values of impedance, calculated by the fitting program, are marked by empty circles.

In the case of spectra registered at 700 °C, the coefficient α attained a value between 0.54 and 0.64, which demonstrates the significant participation of the diffusional impedance. Unfortunately, the spectra were rather featureless, and the standard deviation in the case of fitting the EEC from Fig. 7a was practically equal to the precision of the single-frequency measurement, so no improvement of the fit could be expected by fitting more complicated EECs. Two well-separated semicircles are visible in the spectra measured at 600 °C. The semicircle appearing in the high-frequency range

Fig. 4 Optical microscope image of the SDC electrolyte surface with silver deposit formed around the location where the electrode contacted the electrolyte. Experiments were performed at **a** 700 °C and -0.5 V for 12 h; **b** 500 °C and -0.5 V for 16 h; **c** 350 °C and -0.5 V for 60 h; and **d** 600 °C and -0.005 V for 60 h. The numbers 1–5 denote regions with different silver deposit microstructures



(left part of the spectra in Fig. 6b) represents the impedance of the electrolyte; the semicircle appearing in the low-frequency range (right part of the spectra in Fig. 6b) represents the impedance of the interfacial reaction. In all cases, it was possible to fit the impedance data with the equation describing the equivalent electrical circuit from Fig. 7b, except for the first spectrum. In all cases, the standard deviation of the fit was below 0.01, which means that the assumed EEC describes the measured data well. Again, the electrode reaction is represented by a single semicircle; however, in this case, the coefficient α attained a value between 0.70 and 0.89, characteristic rather for a charge-transfer process.

Generally, the impedance of the electrode decreased over time, which is manifested as a decrease in the diameter of the semicircles visible in the spectra over time. Evidently, this is caused by an increase in the area of the electrode and the tpb length. For this reason, the range of frequency was tentatively restricted on the low-frequency side, since one condition for

the application of EIS is the stability of the measured system during spectrum acquisition. In the case of the measurements performed at 600 °C, the first semicircle was interpreted as the semicircle representing the impedance of the electrolyte; at 700 °C, this could have been visible only at a much higher frequency.

In the experiments performed at 500 °C, only part of the semicircle connected with the impedance of the electrolyte and only part of the semicircle connected with the electrode reaction are visible, and the impedance data are strongly scattered. Hence, in this case, the EEC from Fig. 7b was also used; however, the errors of the parameters calculated based on the fit were very high. The only impedance parameter that could be determined in the case of the experiments performed at 500 °C was the resistance of the electrolyte.

Figure 9 shows the example of the comparison of the polarization resistance calculated from the DC measurements

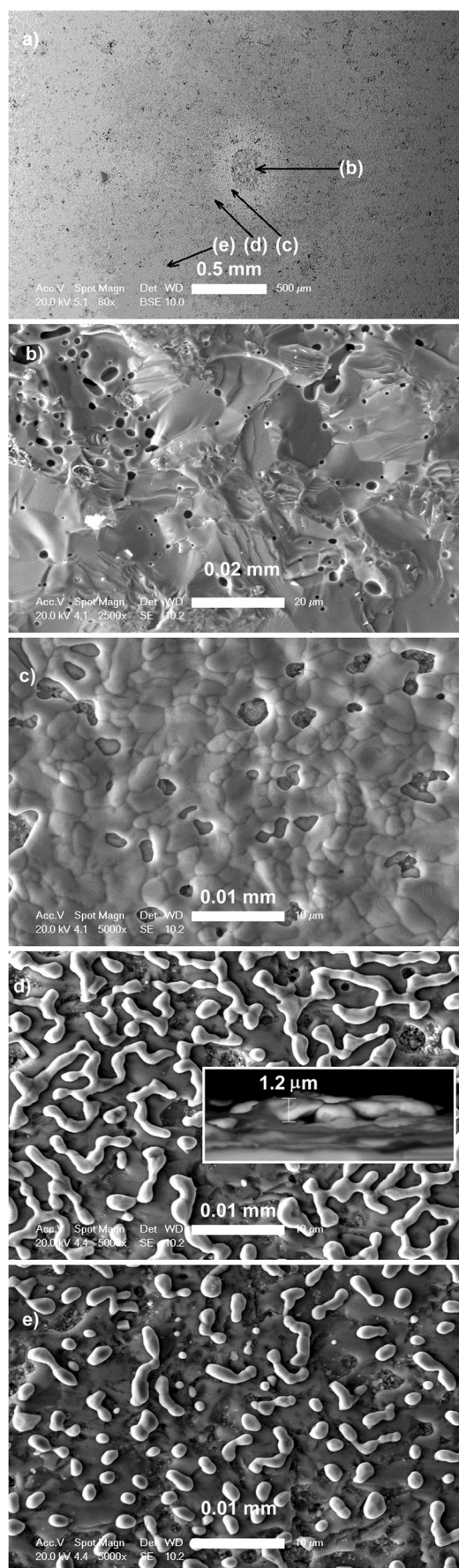


Fig. 5 SEM (SE) image of the SDC electrolyte surface microstructure with a silver deposit formed around the polarized electrode at -0.5 V and 600 °C for 1 h (**a–b**), together with SEM images of the SDC surface in the characteristic regions marked with the letters (**b**)–(**e**). Isolated holes in this silver deposit appeared in region 3, exposing the electrolyte surface (**c**). Region 4 consisted of elongated silver islands with varied thickness from 0.5 to 1.2 μm (*inset*) forming a network on the electrolyte surface (**d**). Isolated small silver islands, either circular or irregular in shape, were scattered over region 5 (**e**). The locations at which the SEM pictures shown in Fig. 5b–e were recorded are marked in Fig. 5a with the same letters. In Fig. 5d, the microstructure of the cross-section of the presented area is shown in the inset

as $R_p = U/I$ and from the impedance data using the following equation:

$$R_p = R_0 + R_1 + R_2 \quad (3)$$

for the experiment performed at 600 °C under a polarization of -0.2 V.

Equation (3) is valid not only for the EECs from Fig. 7b but also for the EEC from Fig. 7a, setting $R_2=0$. It can be seen that the agreement between the polarization resistance calculated from DC and AC measurements is excellent, which confirms that the choice of the EEC was correct. For the experiments performed at 700 °C, the agreement was poorer, which was probably due to the significant participation of diffusional impedance in the electrode impedance at that temperature, as suggested by the EIS data. The polarization resistance calculated from AC data was 10–15 % higher than the value calculated from DC data. In the experiments performed at 500 °C, it was impossible to calculate R_p in most cases due to the high scatter of the impedance data. In the case of the EEC from Fig. 7a, the electrolyte resistance R_e is equal to R_0 ; for the EEC from Fig. 7b, it can be expressed by the following equation:

$$R_e = R_0 + R_1 \quad (4)$$

Based on Eqs. (3) and (4), it was possible to divide the polarization between the resistance of the electrolyte and the charge transfer resistance of the electrode reaction. An example of such division in the case of the experiment performed at 600 °C is presented in Fig. 10. It can be seen that the ratio of charge transfer polarization decreases with time. Both the decrease in electrolyte resistance and the decrease in charge

Table 1 Examples of atomic ratios at the surface of SDC electrolyte in different regions from EDX measurements

| Region | Element, atomic ratio (%) | | | |
|--------|---------------------------|------|------|-----|
| | O | Ag | Ce | Sm |
| 1 | 56.9 | 0.8 | 33.9 | 8.4 |
| 3 | 7.5 | 61.0 | 25.7 | 5.8 |
| 4 (Ag) | – | 89.7 | 8.0 | 2.3 |

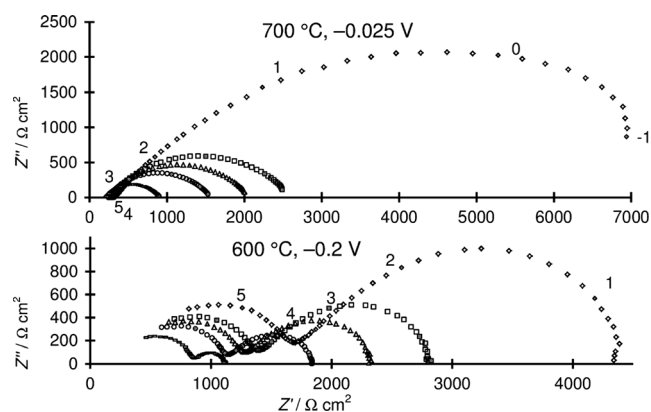


Fig. 6 Examples of the EIS spectra recorded at 700 °C/−0.025 V and at 600 °C/−0.2 V. Spectra registered immediately after applying potential (diamonds), after 22.5 min (squares), after 45 min (triangles), after 90 min (circles), and after 360 min (rectangles). The numbers near the symbols denote the logarithm of frequency

transfer resistance may be ascribed to the increase in the perimeter of the electrode. This progression of change in the ratio of both resistances suggests that charge transfer resistance changes faster with the electrode dimension than with electrolyte resistance.

Discussion

It is still unclear what kind of force moves the silver atoms along the surface. The concept of electron wind impelling the silver atoms to move, proposed by Ho and Huntington [31], fails to explain the movement of such a large mass, as proved by Mosialek et al. [19].

Based on the data of Lu and Zhu [32], Mosialek et al. [20] showed that the sublimation of silver from the wire electrode cannot explain such massive movement of silver at such a relatively low temperature. This conclusion was confirmed by an experiment in which the current was passed between two LSCF electrodes at a potential difference of 0.5 V, with the silver electrode touching the electrolyte halfway between them, but not connected to the potentiostat. This experiment was performed for over 4 h at 600 °C. No silver deposit was found; the current was constant (250 μ A) during the whole experiment (Fig. 11a).

Another possibility is that the negative polarization of the working electrode increases the rate of silver evaporation.

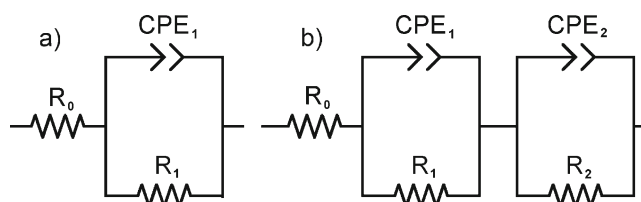


Fig. 7 Equivalent electrical circuits applied in the interpretation of the impedance data

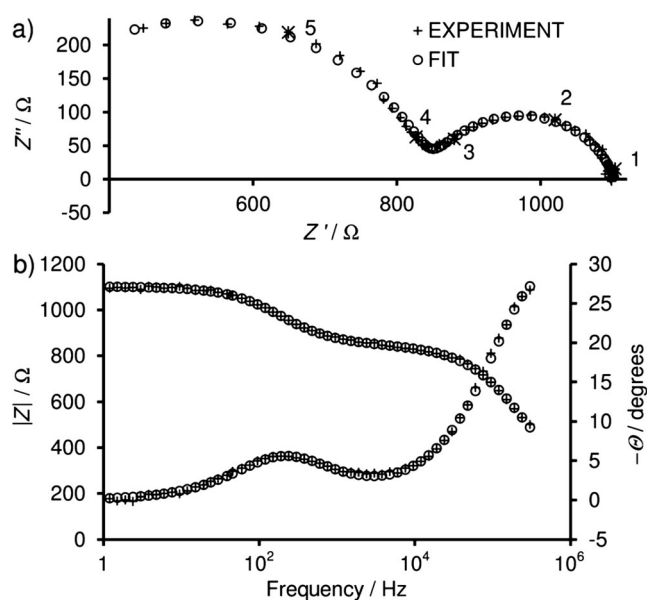


Fig. 8 An example of the fit of the EEC from Fig. 8a to the measured data. The numbers near symbols denote the logarithm of frequency. Nyquist plot (a) and Bode plot (b)

However, the control experiment performed with the two-electrode set-up showed that after 24 h, no silver deposit had appeared at the surface of the electrolyte when the working electrode was maintained at −0.9 V, but separated from the surface by a small gap so that there was no current flow.

To be sure that the source of silver in the deposit is the working electrode and not the counter electrode or the reference electrode, the experiment was performed at 600 °C for 12 h; during which, both electrodes, made of LSCF, were placed on the same side of the electrolyte. In this case, one of the LSCF electrodes served as the counter electrode, the other as the reference electrode. The working electrode was a silver electrode placed midway between the LSCF electrodes. The silver deposit found afterwards on the electrolyte surface was similar to the deposits obtained with the three silver electrodes (Fig. 11b).

The growth of the deposit is undoubtedly connected with the flow of current; only a few very small crystallites are formed around the electrode when the current does not flow. However, in all experiments, the amount of silver transported from the silver wire electrode to the surface of the electrolyte

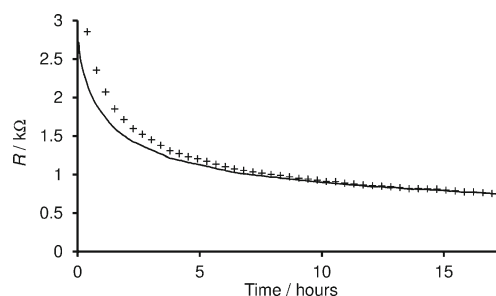


Fig. 9 Comparison of polarization resistance calculated from the DC (line) and AC (plus sign) data

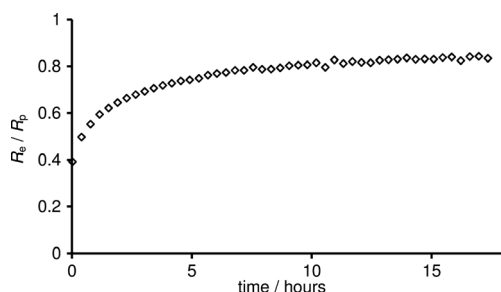


Fig. 10 The ratio of electrolyte resistance to polarization resistance for 600 °C/−0.2 V

was small in comparison with the charge that had flowed in the system. For deposits formed at higher temperatures and

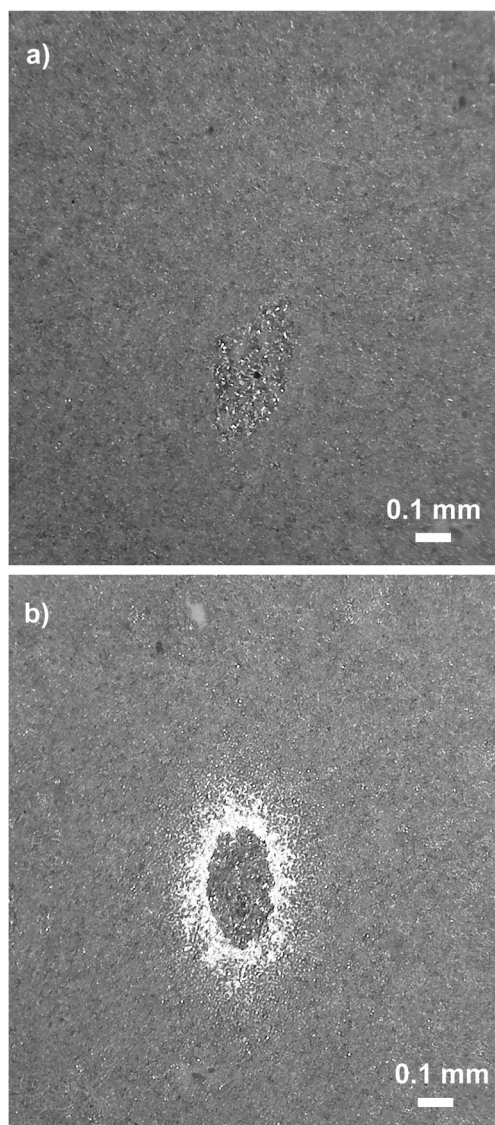


Fig. 11 The optical microscope image of the SDC electrolyte surface: **a** the location where the silver electrode touched the electrolyte after 4 h; during which time, the current was passed between two LSCF electrodes at the potential difference 0.5 V; **b** with the silver deposit formed around the polarized electrode at −0.5 V and 600 °C for 12 h

polarizations, it was possible to estimate the mass of the deposit from microscopic observations. This mass was always less than 1 % of the mass calculated from the charge, assuming that the flow of one electron causes the movement of one silver atom. The rate of growth of the deposit is not even proportional to the current density. Simple derivation shows that, had this rate been proportional to the current, it would have increased constantly. Contrary to expectations, in several cases (see Figs. 3a and 12a), the current stabilized after some time at a constant value, which means that the growth rate of the deposit decreased to zero. This suggests that there is another factor acting opposite to the influence of the current (decreasing the growth rate) whose influence on the current is greater in proportion to the size of the deposit. This potential factor might be evaporation from the deposit, which should be proportional to the deposit area. However, the data from the literature [32] seem to preclude this possibility.

An interesting observation was made during the experiment in which the electrode was polarized alternately by two different negative potentials −0.2 and −0.05 V (Fig. 12a). Figure 12b shows the course of the current over time during the period when the current was stabilized at a constant value. Following an instantaneous change in potential to the more negative value, one might expect an instantaneous increase in the absolute value of the current, followed by an exponential decay. However, after such an instantaneous increase, the current proceeded to increase continuously. When the potential was reset to the initial value of

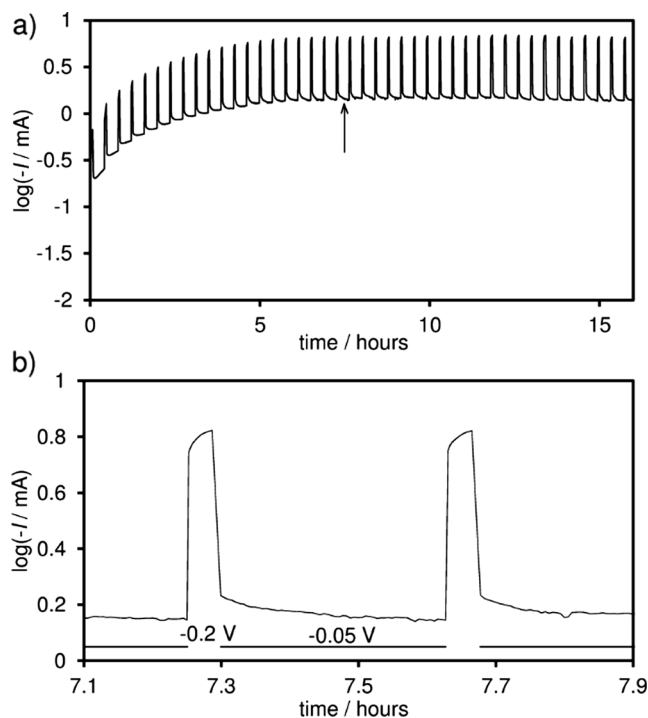


Fig. 12 The course of the current over time in the experiment in which the electrode was polarized alternately by two different negative potentials, −0.2 and −0.05 V (**a**), and the magnification of the plot showing the details of the current changes (**b**)

−0.05 V, the instantaneous fall in the absolute value of current was followed by a slow decrease, instead of the expected exponential increase. If the increase/decrease in current at the constant potential is caused by the increase/decrease in the electrode area, such behavior can be explained, assuming that the actual area of the electrode is the result of the equilibrium between two processes: growth of the electrode area due to the flow of current and shrinkage of the electrode area due to another process (possibly evaporation) whose rate is proportional to the area of the deposit.

Conclusions

There is no way to prevent the migration of silver by lowering overpotential. Silver migration occurs at any negative potential between −0.005 and −0.5 V.

Nor does lowering the temperature help to prevent silver migration. This process occurs at any temperature at which the electrolyte works as an ionic conductor (350–700 °C).

There are two processes influencing the growth of the silver deposit. The first causes an increase, the second a decrease, in the deposit mass; the final deposit mass is the result of the balance of both. The increase of the deposit depends on the current flowing in the system: the greater the current, the bigger the deposit. The decrease in the deposit mass seems to be roughly proportional to its surface area.

Silver is transported from the cathode to the surface of the electrolyte by surface migration, not by the gas phase; however, the reason for the mobility of silver on the surface of an oxide electrolyte is still unclear.

Acknowledgments This work was financially supported by the Polish Ministry of Science and Higher Education (grant No. 6166/B/T02/2010/38). The part of the experiment involving SEM/EDS measurements of SDC was performed in the Accredited Testing Laboratories at the Institute of Metallurgy and Materials Science of the Polish Academy of Sciences.

Open Access This article is distributed under the terms of the Creative Commons Attribution License which permits any use, distribution, and reproduction in any medium, provided the original author(s) and the source are credited.

References

- Baker R, Guindet J, Kleitz M (1997) *J Electrochem Soc* 144:2427–2432
- Liu Y, Mori M, Funahashi Y, Fujishiro Y, Hirano A (2007) *Electrochem Commun* 9:1918–1923
- Simner SP, Anderson MD, Coleman JE, Stevenson JW (2006) *J Power Sources* 161:115–122
- Liu Y, Hashimoto S, Yasumoto K, Takei K, Mori M, Funahashi Y, Fujishiro Y, Hirano A, Takeda Y (2009) *Curr Appl Phys* 9:S51–S53
- Mosiąlek M, Dudek M, Wojewoda-Budka J (2013) *Arch Metall Mater* 58:275–281
- Sakito Y, Hirano A, Imanishi N, Takeda Y, Yamamoto O, Liu Y (2008) *J Power Sources* 182:476–481
- Sholklapper TZ, Radmilovic V, Jacobson CP, Visco SJ, De Jonghe LC (2008) *J Power Sources* 175:206–210
- Dudek M, Mosiålek M, Mordarski G, Socha RP, Rapacz-Kmita A (2011) *Arch Metall Mater* 56:1249–1255
- Li Q, Sun L-P, Huo L-H, Zhao H, Grenier J-C (2011) *J Power Sources* 196:1712–1716
- Su R, Lü Z, Jiang SP, Shen Y, Su W, Chen K (2013) *Int J Hydrog Energy* 38:2413–2420
- Zhou W, Ran R, Shao ZP, Cai R, Jin WQ, Xu NP, Ahn J (2008) *Electrochim Acta* 53:4370–4380
- Su R, Lü Z, Chen K, Ai N, Li S, Wei B, Su W (2008) *Electrochem Commun* 10:844–847
- Guo Y, Liu Y, Cai R, Chen D, Ran R, Shao Z (2012) *Int J Hydrog Energy* 37:14492–14500
- Jaiswal A, Wachsman E (2006) *Solid State Ionics* 177:677–685
- Camaratta M, Wachsman E (2007) *Solid State Ionics* 178:1242–1247
- Camaratta M, Wachsman E (2007) *Solid State Ionics* 178:1411–1418
- Nielsen J, Jacobsen T (2008) *Solid State Ionics* 178:1769–1776
- Nielsen J, Jacobsen T (2007) *Solid State Ionics* 178:1001–1009
- Mosiålek M, Bielańska E, Socha RP, Dudek M, Mordarski G, Nowak P, Barbasz J, Rapacz-Kmita A (2012) *Solid State Ionics* 225:755–759
- Mosiålek M, Dudek M, Nowak P, Socha RP, Mordarski G, Bielańska E (2013) *Electrochim Acta* 104:474–480
- Sasaki K, Hosoda K, Lan TN, Yasumoto K, Wang S, Dokiya M (2004) *Solid State Ionics* 174:97–102
- Jiménez R, Klöidt T, Kleitz M (1997) *J Electrochem Soc* 144:582–585
- Tomczyk P, Żurek S, Mosiålek M (2009) *J Electroceram* 23:25–36
- Jacobsen T, Bay L (2002) *Electrochim Acta* 47:2177–2181
- Jacobsen T, Zachau-Christiansen B, Bay L, Juhl Jørgensen M (2001) *Electrochim Acta* 46:1019–1024
- Mosiålek M, Dudek M, Michna A, Tatko M, Kędra A, Zimowska M (2014) *J Solid State Electrochem*. doi:10.1007/s10008-014-2457-4
- Mosiålek M, Nowak P, Dudek M, Mordarski G (2014) *Electrochim Acta* 120:248–257
- James F, Roos M (1975) *Comput Phys Commun* 10:343–367
- Simka W, Mosiålek M, Nawrat G, Nowak P, Żak J, Szade J, Winiarski A, Maciej A, Szyk-Warszyńska L (2012) *Surf Coat Technol* 213:239–246
- Mosiålek M, Mordarski G, Nowak P, Simka W, Nawrat G, Hanke M, Socha R, Michalska J (2011) *Surf Coat Technol* 206:51–62
- Ho PS, Huntington HB (1966) *J Phys Chem Solids* 27:1319–1329
- Lu ZG, Zhu JH (2007) *Electrochem Solid-State Lett* 10:B179–B182